Interactions between plant RING-H2 and plant-specific NAC (*NAM*/*ATAF1/2*/*CUC2*) proteins: RING-H2 molecular specificity and cellular localization

Krestine GREVE, Tanja LA COUR, Michael K. JENSEN, Flemming M. POULSEN and Karen SKRIVER[1]

Institute of Molecular Biology, University of Copenhagen, Øster Farimagsgade 2A, 1353 Copenhagen K, Denmark

Numerous, highly conserved RING-H2 domains are found in the model plant *Arabidopsis thaliana* (thale cress). To characterize potential RING-H2 protein interactions, the small RING-H2 protein RHA2a was used as bait in a yeast two-hybrid screen. RHA2a interacted with one of the plant-specific NAC [*NAM* ('no apical meristem'), *ATAF1/2*, *CUC2* ('cup-shaped cotyledons 2')] transcription factors, here named ANAC (abscisic acid-responsive NAC). The core RING-H2 domain was sufficient for the interaction. The ability of 11 structurally diverse RING-H2 domains to interact with ANAC was then examined. Robust interaction was detected for three of the domains, suggesting multi-specificity for the interaction. The domains that interacted with ANAC contain a glutamic acid residue in a position corresponding to a proline in many RING-H2 domains. Conversion of this glutamic acid residue into proline in RHA2a decreased its ability to interact with ANAC, most likely by changing the interaction surface. This suggested that a short, divergent region in RING-H2 domains modulate interaction specificity. ANAC contains a degenerate bipartite nuclear localization signal (NLS), while RHG1a, also identified as an ANAC interaction partner, contains a basic NLS. Both signals localized β-glucuronidase reporter fusions to the nucleus. N-terminally truncated RHA2a also directed nuclear localization, apparently dependent on basic amino acids in the RING-H2 domain. Nuclear co-localization of the RING-H2 proteins and ANAC may enable their interaction *in vivo* to regulate the activity of the ANAC transcription factor.

Key words: abscisic acid-responsive nitrogen assimilation control protein (NAC), cellular localization signal, plant model, RING-H2 target protein, ubiquitination pathway.

INTRODUCTION

The RING-finger domain [1] is a specific type of zinc finger that binds two zinc ions using a defined pattern of cysteine (C) and histidine (H) in a 'cross-brace' structure. C_3HC_4 (RING-HC) and $C_3H_2C_3$ (RING-H2) are the most common RING domains. Other variants such as the U-box show sequence similarity with the RING domains, suggestive of a shared fold, despite the lack of several of the signature cysteine and histidine [2]. The widespread occurrence of proteins with RING and variant RING domains, and their association with human and plant diseases [3–6], has prompted interest in these domains and their parent proteins.

RING-domain proteins generally function in protein–protein interactions, often as part of large regulatory protein complexes [7]. They are found throughout the cell, and in mammalian systems they are involved in biological processes such as development, oncogenesis and apoptosis. At the molecular level they may be involved in transcriptional regulation, vesicular transport and peroxisomal biogenesis. Recently most focus on RING proteins has been on their roles in protein degradation through the ubiquitination pathway [8]. Many RING proteins function as E3 ubiquitin ligases that direct ubiquitination and subsequent destruction of specific target proteins. In general, RING-HC domains have been found in single polypeptide E3 ligases, which bind an E2 (ubiquitin-conjugating) enzyme through the RING-HC domain and a target substrate mainly through a region outside the RING-HC domain. In contrast, RING-H2 proteins are often associated with multi-subunit E3 ligases such as the SCF (Skp1.CUL1.F-box protein) complex in which they may not be the primary binding site for target substrates [9].

Plant RING proteins are also involved in ubiquitination pathways. The RING domain of PRT1 is required for degradation of short-lived proteins with a specific N-terminal amino acid as part of the N-end rule ubiquitination pathway [10]. Plant RING proteins have recently been shown to function as E3 ubiquitin ligases [5,11,12]. The most studied plant RING protein is *Arabidopsis thaliana* (thale cress) COP1 (constitutive photomorphogenic 1), which functions as a repressor of photomorphogenesis [13]. COP1 may function by regulating the level of its interaction partner, the bZIP (basic domain/Leu zipper) transcription factor HY5 (hypocotyl complementation group 5), via the proteasome degradation pathway [14]. The RING-H2 protein, CIP8, also an interaction partner of COP1, functions as an E3 ubiquitin ligase and promotes ubiquitin attachment to HY5 [12]. Recently the RING-HC protein SINAT5 [SINA (seven in absentia) of *Arabidopsis thaliana* 5 (located on chromosome 5)]

Abbreviations used: ABA, abscisic acid; AD, GAL4 activation domain; BD, GAL4 DNA-binding domain; CIP8, COP1 (constitutive photomorphogenic 1)-interacting protein 8; E2, ubiquitin-conjugating enzyme; E3, ubiquitin ligase; EF-1a, elongation factor 1a; EST, expressed sequence tag; GA, gibberellic acid; GUS, β-glucuronidase; His_6, hexahistidine; IEEHV, immediate early equine herpes virus; JA, jasmonic acid; MBP, maltose-binding protein; NAC, *NAM* ('no apical meristem')/*ATAF1/2*/*CUC2* ('cup-shaped cotyledons 2'); ANAC, abscisic-acid-responsive NAC; NES, nuclear export signal; Ni-NTA, Ni^{2+}-nitrilotriacetate; NLS, nuclear localization signal; PAR, 4-(2-pyridylazo)resorcinol; PHD, plant homeodomain; PMPS, *p*-hydroxymercuriphenylsulphonate; RFP, Ret finger protein; RT-PCR, reverse-transcription PCR; SCF, Skp1.CUL1.F-box protein; SD, synthetic drop-out; SINAT5, SINA (seven in absentia) of *Arabidopsis thaliana* 5 (located on chromosome 5).

[1] To whom correspondence should be addressed (e-mail ks@apk.molbio.ku.dk).

was shown to promote ubiquitination and degradation of the transcription factor NAC1 [NAC is derived from the names of the founder genes *NAM* ('no apical meristem'), *ATAF1/2* and *CUC2* ('cup-shaped cotyledons 2')]. The *NAC1* gene is induced by the plant hormone auxin, and SINAT5 may thus down-regulate auxin signals in plants [15].

RING domains can function as autonomous protein modules, which physically and functionally interact with other proteins [16] and may bind different protein partners through different zinc-binding regions. Although this suggests that RING domains bind an array of proteins, most of the RING-domain partners identified so far are themselves RING proteins or E2 enzymes [7,9]. We have described a large family of *Arabidopsis* RING-H2 proteins characterized by the stringent consensus sequence $CX_2CX_{14-15}CXH\ X_2HX_2\ CX_3\ WX_{6-8}CPXC$ [17] (amino acids are given in the one-letter code; 'X' means unknown or other amino acid). To analyse their properties and potential interaction specificity, we used the small RING protein RHA2a, which contains a RING-H2 as the only distinct structural domain, as bait in a two-hybrid screen. This identified the RHA2 interactor ANAC (abscisic acid-responsive NAC), a member of the plant-specific NAC transcription factor protein family. The assaying of ANAC interactions with a spectrum of structurally similar RING-H2 domains allowed an analysis of the specificity determinants in the RING-H2 domains for interactions with ANAC. The implications of the interactions between the *Arabidopsis* RING-H2 proteins and NAC transcription factors are discussed.

MATERIALS AND METHODS

Identification and analysis of predicted RING-H2 and RING-HC proteins

Searches in the expressed sequence tag (EST) and non-redundant databases were performed using BLAST [18] and selected domains as search strings. Predicted sequences were examined for similarity to known protein sequences by BLAST, for domain architectures and intrinsic sequence features such as transmembrane regions, coiled coils and signal peptides by SMART [19], and for sorting signals by PSORT [20]. Secondary structure was predicted by comparison of the results from the Jnetpred, PSIPRED and the PHD programs obtained from the Meta-Server [21]. EST cDNA clones of interest were acquired from the *Arabidopsis* Biological Resource Center (Ohio State University, Columbus, OH, U.S.A.).

Yeast two-hybrid screens and interaction assays

The bait genes used for two-hybrid screens and assays were expressed as fusion to the GAL4 DNA-binding domain (BD) from the pGBKT7 vector (Clontech). A summary of bait plasmid constructs and PCR primers used to generate these is given in Table 1. The $Glu^{103} \rightarrow Pro$ substitution was introduced into the RHA2a (38–155)–BD construct using primers 5′-GAAGAGGTGAGGAAGCTGCCATGTCGACACGTGTTCCAC and 5′-GTGGAACACGTGTCGACATGGCAGCTTCCTCACCTCTTC, and the $Cys^{89} \rightarrow Ser$ substitution was introduced into RHA2a using primers 5′-GCGGCTCCGATTGTGTTGTGTCTTTGTCGAAGTTAAAGGAAGG and 5′-CCTTCCTTTAACTTCGACAAAGACACAACACAATCGGAGCCGC. ANAC was cloned into pGBKT7 using the upstream *Nde*I linker primer 5′-CCATGTCAGCCATATGGGTATCCAAGAAA and the downstream *Bam*HI linker primer 5′-CGACTGGGATCCTTATTATCACATAAACCCAAACCC. The cDNA corresponding to *Arabidopsis* At5g53300 and encoding the E2 enzyme previously named UBC10 was amplified using the upstream

Table 1 Primers used for RING-H2–GAL4-BD two-hybrid bait constructs

RING-H2 domains were cloned into pGBKT7 to produce the RING-H2 fragments shown (residue numbers in parentheses) fused to BD.

Construct	Primer sequence
RHA1a(45–159)–BD	TAGAATTCGACCACAACGAGACCTCTGGA TAGGATCCTTAGTTGGTACTTTCCACTTC
RHA2a(1–155)–BD	TAGAATTCATGGGGCTACAAGGTCAGCTA TAGGATCCTCAGTGGAGAGAGAAACACGA
RHA2a(38–155)–BD	TAGAATTCACCTCTAAATCAAATCCTAAT TAGGATCCTCAGTGGAGAGAGAAACACGA
RHA2a(77–155)–BD	ATATATATACATATGGGTGACGGAGGTGGTGGC TAGGATCCTCAGTGGAGAGAGAAACACGA
RHA2b(53–147)–BD	TAGAATTCGCCGACCAGCTCAACCTAAAT TAGGATCCTCAATGAGATGATGCAGTAGA
RHA3a(56–185)–BD	TAGAATTCCGGTTTACAGCCGGAGGA TAGGATCCTTAAGGAAGAAACGTAGGAAT
RHA3b(54–200)– BD	TAGAATTCCGTCTCACCGGAGTT TAGGATCCTCAAGGAAGAAAAGCAGGAAT
RHF1a(21–115)–BD	TAGAATTCGCCATTGGTTCTTCGTCT TATATATGTCGACTTATATATTCCTGGTTTTCAA
RHF2a(1–106)–BD	TATCCCGGGGATGGAGGGAGCGGGAGAGAC ATATATATACTGCAGTTAGGTGGCATTTCTAGTTGG
RHG1a(584–691)–BD	TATATACCCGGGGATGCGACTTGATGTGGAC ATATATATACTGCAGTTATGCTATCCTCCGCTTCTT
RHG1a(502–691)	ATATATATACCCGGGGGCTTACTCGAGAGCAGGT ATATATATACTGCAGTTATGCTATCCTCCGCTTCTT
RHY1a(150–250)–BD	TAGAATTCTCATTTCATTCTATAGATGGA TAGGATCCCTATTCCTTTGCTATGGCTCT
AT1g55530(175–306)–BD	TAGAATTCTTAGGTGACTATTTCATT TAGGATCCTTATTGGCGCCGGTTTCCATC
ATL4(69–192)–BD	TATATATACATATGGTCGCAACCGTA TATATATACTGCAGTTATCCGATTTCGAGACGGAA

*Eco*RI linker primer 5′-ATGAATTCATGGCGTCGAAGCGGATC and the downstream *Xho*I linker primer 5′-ATATATCTCGAGTTAGCCCATGGCATACTT. Two-hybrid screens were carried out with *Saccharomyces cerevisiae* strain PJ69-4A (*MATa*, *trp1-901*, *leu2-3*, *112 ura3-52*, *his3-200*, *gal4*, *gal80*, *LYS2::GAL1-HIS3*, *GAL2-ADE2*, *met2::GAL7-lacZ*) by sequential transformation of PJ96-4A. The cDNA library used for the screen was obtained from the *Arabidopsis* Biological Resource Center and was constructed in a pACT vector from random-primed mRNA isolated from mature *Arabidopsis* leaves and roots. The yeast mixture was plated on synthetic dropout (SD) medium lacking tryptophan, leucine, histidine and adenine. Positive colonies appearing within 6 days of the screen and activating the *HIS3* and *ADE2* reporter genes were subsequently tested for β-galactosidase activity. The interactions were initially confirmed by co-transformation of isolated bait and library plasmids. For additional quantitative interaction assays plasmid combinations were transformed into yeast, and *o*-nitrophenyl β-D-galactopyranoside assays performed (Clontech Yeast Protocols Handbook).

To extract protein yeast cells in liquid culture (SD, −Trp, −Leu) were harvested at an attenuance (D_{600}) of 0.4–0.5, resuspended in 8 M urea/5% (w/v) SDS/0.1 mM EDTA/40 mM Tris/HCl (pH 6.8)/0.4 mg/ml Bromophenol Blue buffer, heated at 70 °C for 10 min and mixed with glass beads. After centrifugation at 22000 ***g*** for 5 min, the pellet was boiled for 5 min, mixed and centrifuged at 22000 ***g*** for 5 min. The supernatants were subjected to SDS/PAGE, followed by protein

gel-blot analysis using GAL4 monoclonal antibodies (Clontech, Palo Alto, CA, U.S.A.).

Expression and purification of recombinant RHA2a and ANAC proteins and generation of polyclonal antibodies

An RHA2a fragment corresponding to full-length RHA2a protein was synthesized by PCR with an upstream *Eco*RI linker primer 5′-TATATAGAATTCATGGGGCTACAAGGTCAG-CTA and a downstream *Xho*I linker primer 5′-TATATACTC-GAGTCAGTGGAGAGAGAAACACGA and cloned into the pMAL-c2 expression vector (New England Biolabs). The $Glu^{103} \rightarrow$ Pro substitution was introduced into RHA2a using the primers 5′-GAAGAGGTGAGGAAGCTGCCATGTCGACA-CGTGTTCCAC and 5′-GTGGAACACGTGTCGACATGG-CAGCTTCCTCACCTCTTC. Recombinant maltose-binding protein (MBP) and RHA2a–MBP fusion proteins were purified by amylose–agarose affinity chromatography. For the generation of polyclonal antibodies, 1.5 mg of freeze-dried MBP–RHA2a (1–155) was resuspended in 0.3 ml of Freund's complete adjuvant before injection into rabbits, and the antiserum was purified on MBP–RHA2a(1–155) bound to amylose–agarose. DNA fragments encoding both full-length ANAC (residues 1–317) and three C-terminal deletions (residues 1–138, 1–161 and 1–168) were PCR-amplified by using the upstream *Nde*I linker primer 5′-CCATGTCAGCCATATGGGTATCCAAGAAACTG and the downstream *Bam*HI linker primers 5′-CGACTGGGATCC-TTATTATCACATAAACCCAAACCC, 5′-CGACTGGGAT-CCTTATTAACGATACTCATGCATGAT, 5′-CGACTGGG-ATCCTTATTACTTGTATATTCGACATAG and 5′-CGAC-TGGGATCCTTATTATTTTTGTGCACTTGATTGC. These fragments were cloned into the pET15b expression vector (Novagen). The resulting hexahistidine (His_6)-tagged proteins, named His_6-ANAC(1–317), His_6-ANAC(1–168), His_6-ANAC (1–161) and His_6-ANAC(1–138), were purified on Ni^{2+}-nitrilo-triacetate (Ni-NTA) as described by the manufacturer (Qiagen) and dialysed before use.

CD spectral analysis of His_6-ANAC(1–168)

CD of His_6-ANAC(1–168) was recorded in the far-UV region between 190 and 250 nm at 25 °C. Recordings were performed with a Jasco J-810 spectropolarimeter equipped with a quartz cell with a path length of 1 cm. The sample contained a protein concentration of 1 μM in 5 mM sodium phosphate buffer (pH 7.5)/3 mM NaCl. For each analysis, 20 scans were performed and subsequently averaged. Results were expressed in terms of mean residue ellipticity (degrees $\cdot$ cm^2 $\cdot$ $dmol^{-1}$). Noise reduction of the averaged spectra was done using the FFT-filter from the Jasco Spectra Analysis software. Secondary-structure predictions were performed using the DICROPROT program (http://antheprot-pbil.ibcp.fr/).

Determination of zinc content

The zinc-binding stoichiometry of purified MBP-RHA2a recombinant proteins was determined spectrophotometrically [22]. To reduce contamination with metal ions, solutions were passed through a Celex-100 column (Bio-Rad Laboratories) before use. Thiol groups present in 3 μM protein were allowed to react with with *p*-hydroxymercuriphenylsulphonate (PMPS) by the addition of a small volume of 4 mM PMPS, and released zinc was bound by 4-(2-pyridylazo)resorcinol (PAR) present at a concentration of 0.1 mM. Zn^{2+} release was determined indirectly by monitoring the absorbance at 500 nm caused by formation of Zn^{2+}–PAR_2 complex. The molar absorption was determined to be 6.8×10^4 $M^{-1} \cdot cm^{-1}$ at 500 nm, and spectrophotometric measurements were performed using a Hewlett–Packard diode-array model 8452A spectrophotometer. The concentration of protein was determined by amino acid analysis.

In vitro binding assay

In pull-down assays using 1 μM recombinant proteins, His_6-ANAC(1–168) was mixed with MBP–RHA2a(1–155) and incubated for 30 min at room temperature in 50 mM Tris/HCl (pH 7.5)/250 mM NaCl/2 mM $MgCl_2$/0.1 mM $ZnCl_2$/0.2 % Tween 20/10 % (v/v) glycerol/0.2 mg/ml BSA. Ni-NTA resin was added to the reaction mixtures, and incubations continued for 1 h at 4 °C. After washing, protein was released with 1 % SDS and analysed by PAGE followed by Western blotting. After PAGE, proteins were transferred on to a PVDF membrane (Immobilon P; Millipore) and blocked with 1 % (w/v) non-fat dry milk before incubation with anti-MBP–RHA2a. Pig anti-IgG–horseradish peroxidase conjugate (Dako) was used as the secondary antibody and proteins were detected by enhanced chemiluminescence (ECL®; Amersham Pharmacia Biotech).

Nuclear localization assay

β-Glucuronidase (GUS) fusions for nuclear localization studies were made by PCR amplification of target DNA using linker-primers encoding an optimal translation start context [23], and the products were inserted into the *Eco*RI or *Bam*HI and *Sma*I sites of a derivative of expression vector pFM6 [24]. ANAC was amplified using the upstream primer 5′-GTCAGCGG-ATCCAACAATGGGTATCCAAGAAACTG and the down-stream primer 5′-CGACTGCCCGGGCATAAACCCAAAC-CC (encoding residues 1–317). RHG1a was cloned using the upstream primer 5′-ATAGAATTCAACAATGACCATATC-AAACCGGTTA and the downstream primer 5′-TATACCC-GGGTGCTATCCTCCGCTTCTT (residues 614–691) or the upstream primer 5′-ATAGAATTCAACAATGACCATATC-AAACCGGTTA and the downstream primer 5′-TATACCC-GGGCGCGGTGTTCAAGCCTGT (residues 614–685). The RHG1a PCR fragments were cloned after partial digestion with *Eco*RI. Full-length RHA2a (residues 1–155) and two N-terminal deletion mutants (encoding residues 38–155 and 65–155) were cloned using the downstream *Sma*I linker primer 5′-ATATCCC-GGGGTGGAGAGAGAAACACGA and the upstream *Eco*RI linker primers 5′-ATAGAATTCAACAATGGGGCTACAAG-GTCAGCT, 5′-TAGAATTCAACAATGACCTCTAAATCA-AATCCT and 5′-TAGAATTCAACAATGCAGCTTAGTTT-GAATCGG respectively. Double mutation of the RHA2a RING-H2 domain, containing the changes $Lys^{110} \rightarrow$ Asn and $Lys^{111} \rightarrow$ Glu, was performed by PCR-based overlap extension using the internal primers 5′-CGTGTTCCACAATGAGTGTT-TGGAAGGATG and 5′-CTTCCAAACACTCATTGTGGAA-CACGTGTC and the upstream and downstream primers used to amplify residues 65–155 of RHA2a.

Reverse-transcription PCR (RT-PCR) and Northern analysis of expression

Arabidopsis plants were grown in a greenhouse at 21 °C with 18 h light and 6 h dark. For liquid cultures, surface-sterilized *Arabidopsis* seeds were grown for 13 days in Murashige and Skoog [24a] agar in constant light at 21 °C before transfer to conical flasks containing MS liquid medium. Liquid cultures were incubated with shaking at 21 °C and constant light. After 36 h, seedlings were subjected to different treatments for 12 h: 10 μM auxin, 50 μM gibberellic acid (GA), 100 μM abscisic acid (ABA)

or 100 μM jasmonic acid (JA). Tissues were harvested and frozen in liquid nitrogen. Total RNA was isolated by LiCl precipitation, phenol/chloroform extraction and ethanol precipitation followed by DNase treatment in a reaction coupled to RT using oligo-dT primers and murine leukaemia virus (MuLV) reverse transcriptase; 1 μg of mRNA was used, and 5 % of the cDNA products were used for PCR amplification of untreated tissues, and 1 % or 0.5 % was used for hormone-treated and mutant tissue. *Pyrococcus furiosus* DNA polymerase was used for PCR in the following PCR program: 30 min, 95 °C → 30 × (45 s, 94 °C) → 45 s, 45 °C → 3 min, 72 °C) → 15 min, 72 °C → 4 °C. Primer sets were 5′-GTTTCACATCAACATTGTGGTCATTGG and 5′-GAGTACTTGGGGTAGTGGCATCC for EF-1a (elongation factor 1a; constitutively expressed control), 5′-ACGGAAGCACTAAGTTGGATG and 5′-AAACCCACCAACTTGCCCCGA for ANAC, 5′-GCCGTCTTCATCAACCATC and 5′-TGGTCAAACCGAACCAG for RHA2a, and 5′-CCACAAGATGCAGAGCCATGC and 5′-CGCGGTGTTCAAGCCTCTAG for RHG1a. For the RNA Northern analyses, 10 μg of denatured RNA was blotted on to a Hybond N nylon membrane (Amersham Pharmacia Biotech). A ^{32}P-labelled probe of a C-terminal-specific DNA fragment of ANAC was prepared with a High Prime Labelling Kit (Boehringer–Mannheim). Incubation and washing procedures were as described by the manufacturer.

Visualization of three-dimensional structure

WebLab Viewer 3.7 [Accelrys (formerly Molecular Simulations Inc.), San Diego, CA, U.S.A.] was used to display the tertiary structure of the RING-HC domain from immediate early equine herpes virus [IEEHV; Protein Data Bank (Rutgers University, Newark, NJ, U.S.A.) entry 1CHC] and human MAT1 protein (Protein Data Bank entry 1G25).

RESULTS

Domain structure of *Arabidopsis* RING-H2 and RING-HC proteins

Our previous classification of predicted *Arabidopsis* RING-H2 proteins was based mainly on EST information [17]. We therefore performed a revised analysis for RING proteins utilizing the complete *Arabidopsis* genome sequence [25]. RING proteins identified in BLAST searches were evaluated solely for identity and spacing of the metal-binding amino acids, e.g. $CX_2CX_{9-39}CX_{1-3}HX_{2-3}CX_2CX_{4-48}CX_2C$ for the RING-HC type and $CX_2CX_{9-39}CX_{1-3}HX_{2-3}HX_2CX_{4-48}CX_2C$ for the RING-H2 type. The number of RING domains identified by these criteria is similar to those derived from a recent classification of *Arabidopsis* RING proteins [26]. Only domains containing a complete set of eight metal-binding amino acids were included in the subsequent analyses. Most of the predicted RING-H2 proteins belong to groups RHA–RHG [17], with the RING-H2 domain as the only distinct structural domain (Figure 1). Approx. 40 % of these simple proteins were predicted to contain a transmembrane region. A larger fraction of RING-HC proteins was predicted to contain additional well-defined domains (Figure 1), but no unifying function was revealed from the domain analyses.

The RING domain is present in 1.42 % of predicted *Arabidopsis* proteins, but only in 0.70–0.75 % of proteins from other eukaryotes such as the fruitfly *Drosophila melanogaster*, the nematode worm *Caenorhabditis elegans* and the yeast *S. cerevisiae* [25]. Over representation of the RING-H2 domain in *Arabidopsis* compared with *S. cerevisiae* is even more pronounced. Whereas the RING-H2 type constitutes 65 % of predicted *Arabidopsis* RING domains, only 49 % of the yeast RING domains displayed by SMART are RING-H2 domains.

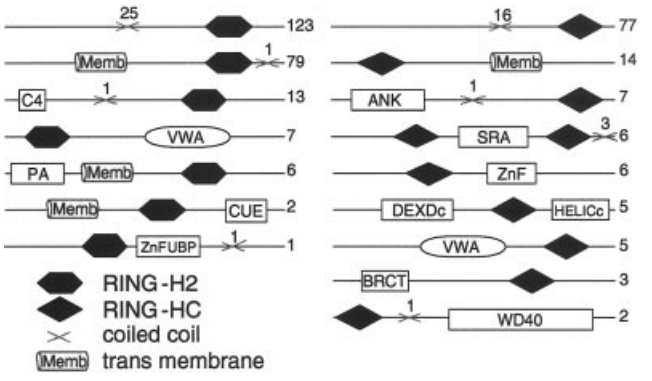

Figure 1 Structural grouping of *Arabidopsis* RING-H2 and RING-HC proteins

Predicted RING proteins were identified by BLAST [18] and analysed for domain architecture, coiled coils and transmembrane regions using BLAST and SMART [19]. The number of proteins with a given domain composition is indicated to the right of their structural outlines, and the number above the outline indicates the number of proteins predicted to contain a coiled coil. Outlines are not drawn to scale, and only the domain composition, not the arrangement of domains along the polypeptide, is shown. The identities of the domains shown by boxes are: C4, Cys_4 zinc finger; PA, protease-associated domain; VWA, von Willebrand factor type A domain; CUE, ubiquitin system component Cue; ZnFUBP, ubiquitin C-terminal hydrolase-like zinc finger; ANK, ankyrin repeats; SRA, SET and RING finger-associated domain; ZnF, zinc-finger domain; DEXDc, DEAD-like helicase superfamily domain; HELICc, helicase superfamily C-terminal domain; BRCT, breast-cancer C-terminal domain; WD40, tryptophan/aspartic acid 40 repeats.

Identification of a NAC protein as a RING-H2-interacting protein

The proliferation of RING-H2 proteins in *Arabidopsis* makes these proteins of interest to plant biology. The small, simple RHA proteins (e.g. RHA1a, RHA1b, RHA2a, RHA2b, RHA3b and RHA3b; [17]) provide an obvious platform to study the interactions, and thereby function, of the RING-H2 domains. To this end, the comparatively highly expressed RHA2a protein was selected as bait in yeast two-hybrid screens for interactions partners. The lack of auto-activation and self-interaction of RHA2a in the two-hybrid assay made this protein amenable as bait. Both RHA2a(1–155)–BD, representing full-length RHA2a fused to the BD of the GAL4 protein, and RHA2a (38–155)–BD, lacking the putative RHA2a N-terminal transmembrane region, were used as baits. The screened cDNA library was from *Arabidopsis* leaf and root mRNAs. Of approx. 4×10^6 transformants, 15 colonies were able to grow on selective medium and expressed β-galactosidase activity. Sequencing revealed that four clones encoded the NAC protein At1g52890, here named ANAC.

The *ANAC* cDNA encodes a protein of 317 amino acids and is a member of the plant-specific NAC [27,28] gene family. Alignment of ANAC with seven *Arabidopsis* NAC proteins shows a high degree of sequence conservation in the N-termini and sequence divergence in the C-termini (Figure 2). The first NAC proteins to be described were *Petunia* NAM [27] and *Arabidopsis* CUC2 [28], which are both important in shoot meristem development. Although there is increasing evidence that NAC proteins are involved in developmental processes, a role for NAC proteins in plant defence has also been implicated [29,30].

ANAC expression

The distribution of *ANAC* mRNA was analysed by RT-PCR using ANAC-specific primers and RNA from different *Arabidop-*

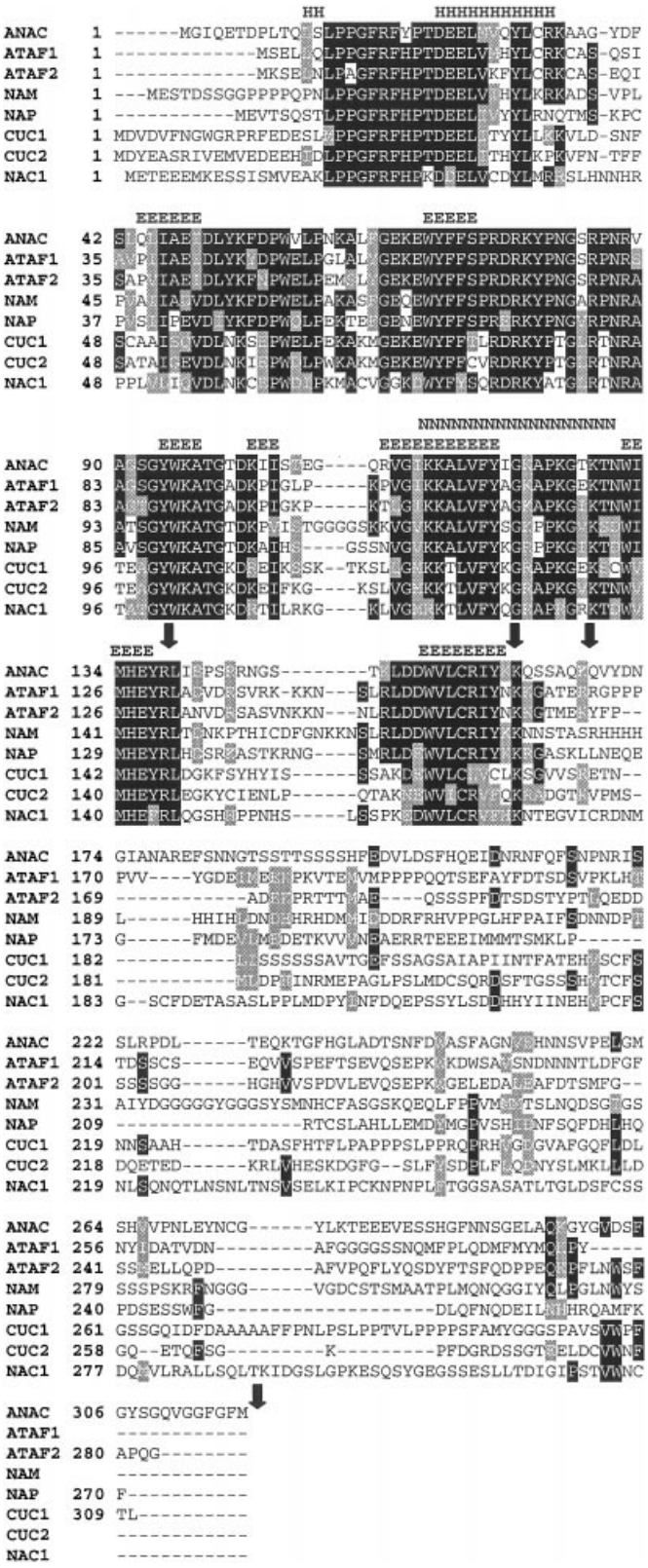

Figure 2 Alignment of ANAC with related NAC proteins from *Arabidopsis*

Alignment of eight *Arabidopsis* NAC proteins with conserved regions in black. The region in ANAC corresponding to the bipartite nuclear localization signal (NLS) in NAC1 [31] is shown by 'N'. Predicted α-helixes are shown by 'H' and strands in β-sheets by 'E'. C-terminal borders of the NAC recombinant proteins produced for the *in vitro* interactions assays (Figure 5C) are shown by an arrow. The sequences shown are: ANAC (the present study); ATAF1 and 2 (accession numbers X74756 and X74755); NAP (accession number NP_56496654); CUC1 and CUC2 [28]; NAC1 [31].

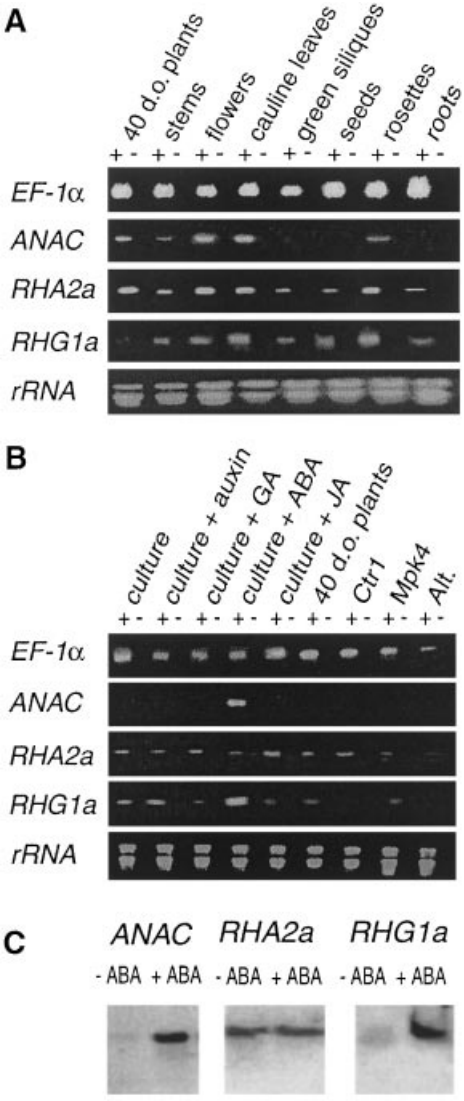

Figure 3 Accumulation of ANAC, RHA2a and RHG1a mRNA and induction by ABA

(**A**) RT-PCR analysis of the expression pattern of the *ANAC*, *RHA2a* and *RHG1a* genes. RNA from *Arabidopsis* tissues was tested in the presence (+) and absence (−) of reverse transcriptase. *EF-1α*, constitutively expressed control. (**B**) RT-PCR analysis of RNA from *Arabidopsis* liquid cultures. Alt., *Alternaria brassicola*-infected plants. *Mpk4* and *Ctr1*, *Arabidopsis* mutants (see the text). To examine for induced mRNA accumulation, only one-fifth (for *ANAC, RHA2a* and *RHG1a*) and one-tenth (*EF-1α*) of the amount of reverse-transcribed DNA used for the reactions shown in (**A**) was used for the reactions shown in (**B**). *rRNA* is RNA template sample stained with ethidium bromide. (**C**) Northern-gel-blot analysis of *ANAC, RHA2a* and *RHG1a* accumulation in liquid culture (left lane) and in liquid culture treated with ABA (right lane).

sis tissues (Figure 3A). RNA from liquid cultures treated with different hormones was included, since hormonal induction has been reported for one of the NAC proteins, NAC1 [31]. The experiment also included RNA from the *Arabidopsis mpk4* [32] and *ctr1* [33] mutants and from plants infected with the fungus

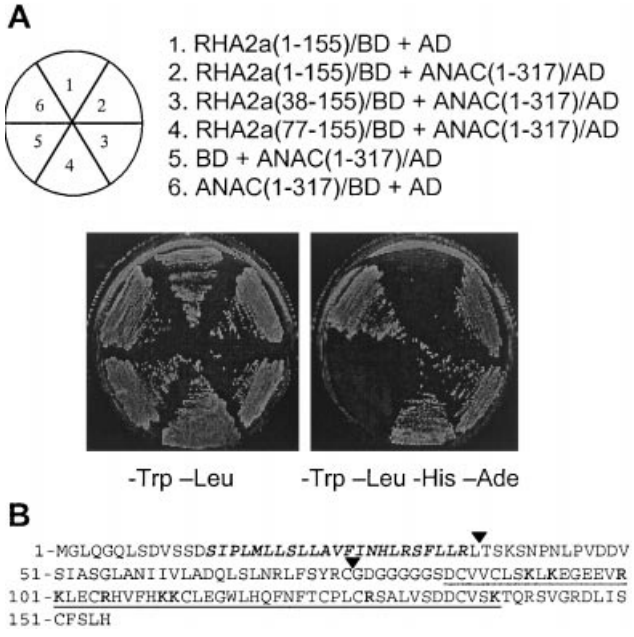

Figure 4 Interactions between RHA2a and ANAC and transcriptional activation by ANAC

(**A**) Yeast two-hybrid assay. Full-length RHA2A, RHA2a(1–155) or N-terminally deleted RHA2a(38–155) and RHA2a(77–155), were cloned into pGBKT7 as in frame fusions with BD. ANAC(1–317) was cloned into pACT in-frame with the AD and in pGBKT7 in-frame with BD. Yeast cells were transformed simultaneously with a combination of the indicated plasmids and streaked on plates lacking Leu and Trp (' — Leu — Trp ') or Leu, Trp, His and adenine (' — Leu — Trp — His — Ade '). The array of yeasts containing the different constructs is indicated by the scheme and numbers at the top. (**B**) Amino acid sequence of RHA2a. Arrows show positions of N-terminal truncation of RHA2a used for the two-hybrid assays in (**A**). The RING-H2 domain is underlined, the hydrophobic region is shown in ***bold italics***, and basic amino acids in the RING-H2 domain, putatively participating in nuclear localization, are shown in **bold**.

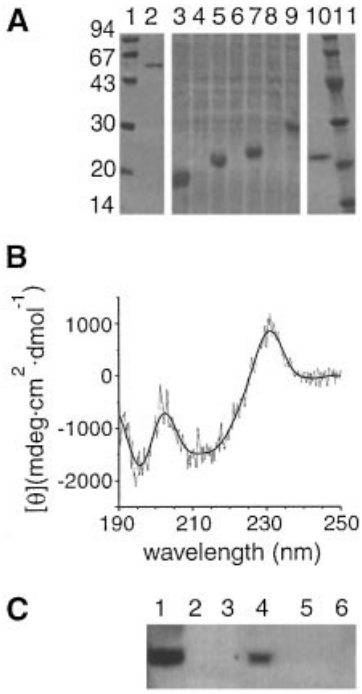

Figure 5 Interaction of RHA2a and ANAC(1–168) recombinant fusion proteins

(**A**) Production and purification of recombinant MBP-RHA2a(1–155) and His_6-ANAC proteins. SDS/PAGE and Coomassie Blue staining of molecular-mass marker (in kDa at the left) (lane 1), purified recombinant MBP-RHA2a(1–155) (lane 2), lysed cells expressing His_6-ANAC(1–138) (lane 3), His_6-ANAC(1–161) (lane 5), His_6-ANAC(1–168) (lane 7), His_6-ANAC(1–317) (lane 9), purified recombinant His_6-ANAC(1–168) (lane 10) and molecular-mass markers (lane 11). Lysed cells before expression of recombinant protein are shown in lanes 4, 6 and 8. (**B**) Far-UV CD spectrum of 1 μM His_6-ANAC(1–168). (**C**) *In vitro* pull-down interaction assays. Affinity-purified recombinant MBP–RHA2a(1–155) or MBP and His_6-ANAC(1–168) were preincubated prior to addition of Ni-NTA resin and centrifugation. SDS/PAGE and Western-blot analysis using anti-MBP–RHA2a(1–155) as primary antibody of the following samples or pellets: MBP–RHA2a(1–155) loaded directly (lane 1), MBP + nickel beads (lane 2), MBP–RHA2a(1–155) + nickel beads (lane 3), His_6-ANAC(1–168) + MBP–RHA2a(1–155) + nickel beads (lane 4), His_6-ANAC(1–168) + MBP + nickel beads (lane 5) and His_6-ANAC(1–168) + nickel beads (lane 6).

Alternaria brassicola. The *mpk4* mutant exhibits constitutive systemic acquired resistance, while *ctr1* exhibits constitutive ethylene responses, including ectopic expression of certain pathogen-inducible genes. RNA from these plants was included to examine *ANAC* expression in response to pathogen infection. A single band of the expected size was obtained in 40-day-old plants, stems, flowers, cauline leaves and rosettes, suggesting a moderately restricted accumulation pattern for *ANAC* mRNA. Furthermore, *ANAC* mRNA accumulated in response to ABA. The level of the phytohormone ABA increases under stress conditions triggering adaptive responses [34]. A similar induction was not seen for the constitutively expressed *EF-1a* gene (Figure 3B). ABA induction of *ANAC* gene expression was confirmed by Northern-gel-blot analysis of untreated and ABA-treated liquid culture (Figure 3C). In contrast, the level of EF-1a mRNA was unaffected by ABA treatment (results not shown). RHA2a mRNA was detected in a wider range of tissues than ANAC mRNA, but the *RHA2a* and *ANAC* genes were co-expressed in several tissues (Figure 3A). Co-expression renders interactions between the corresponding proteins possible. No effect of ABA on *RHA2a* gene expression was detected (Figures 3B and 3C).

RHA2a and ANAC interactions

The interaction between RHA2a and ANAC was initially confirmed by re-transformation of isolated plasmids into yeast and assays for growth on selective medium. This confirmed that RHA2a(1–155)–BD interacted *in vivo* with ANAC(1–317)–AD, representing full-length ANAC fused to the GAL4 activation domain (AD) (Figure 4A). Control experiments using RHA2a (1–155)–BD and AD showed no growth on selective medium. The truncated RHA2a versions, RHA2a(38–155)–BD, lacking the N-terminal hydrophobic region, and RHA2a(77–155)–BD, containing only the RING-H2 domain, were also able to interact with ANAC(1–317)–AD (Figures 4A and 4B). This suggested that the RING domain of RHA2a was sufficient for the interaction with ANAC. Importantly, ANAC(1–317)–AD did not support growth on selective medium. In contrast, ANAC (1–317)–BD grew on the same selective medium, in accordance with previous studies showing that NAC proteins can function as transcriptional activators [31].

RHA2a and ANAC recombinant proteins were used for pull-down experiments to assess interaction *in vitro*. Full-length RHA2a was produced as a fusion to MBP. The MBP-RHA2a (1–155) recombinant protein was soluble, despite the presence of the hydrophobic N-terminal region and was purified by amylose–agarose affinity chromatography (Figures 4B and 5A). Since

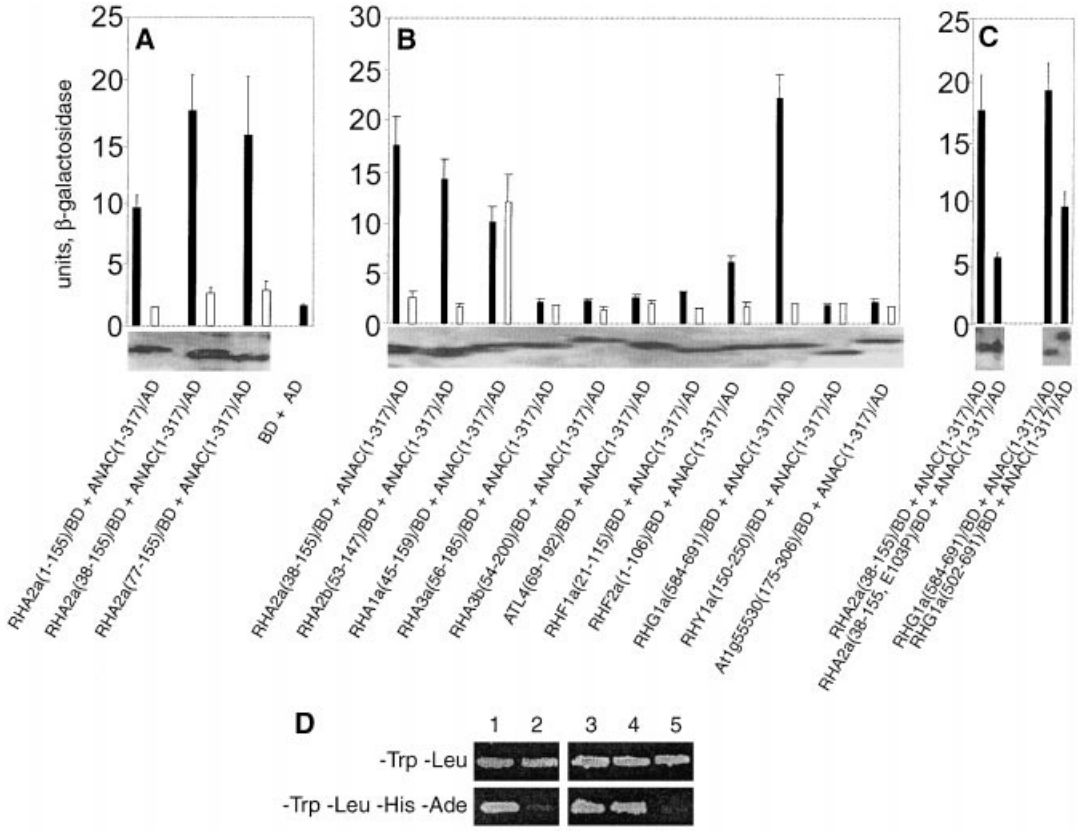

Figure 6 ***In vivo*** **interactions between** ***Arabidopsis*** **RING-H2 domains and ANAC: specificities and determinants of interactions**

(**A**) β-Galactosidase activity of yeast cells co-transformed with an RHA2a–BD construct and an ANAC(1–317)–AD (black bars) or AD (white bars) construct for background comparison. The background β-galactosidase activity level from the BD and AD GAL4 proteins was also monitored (BD + AD, black bar on extreme right). The activity of the yeast transformants was measured by a colorimetric assay. Error bars indicate S.D. values from at least three independent measurements. Expression of the RHA2a–BD constructs in the RHA2a–BD and ANAC(1–317)–AD co-transformations was monitored by Western-blot analysis using GAL4–BD monoclonal antibodies and shown below each data set. (**B**) Similar to (**A**), but using different RING-H2–AD constructs. (**C**) Co-transformation of ANAC(1–317)–AD and the RING-H2–BD construct shown. Expression of the RING-H2–BD proteins was monitored by Western blot for each co-transformation. (**D**) Yeast two-hybrid assay. The yeast cells were co-transformed with the plasmids indicated and allowed to grow for 6 days on plates lacking Leu and Trp (' — Leu — Trp') or Leu, Trp, His and adenine (' — Leu — Trp — His — Ade'). The co-transformations were: ATL4(69–192)–BD and UBC10(1–148)–AD (lane 1); ATL4(69–192)–BD and ANAC(1–317)–AD (lane 2); RHA2a(38–155)–BD and ANAC(1–317)–AD (lane 3); RHA2a(38–155; E103P)–BD and ANAC(1–317)–AD (lane 4); RHA2a(38–155; C89S)–BD and ANAC(1–317)–AD (lane 5).

details of the structural properties of NAC proteins are still lacking, different lengths of ANAC were produced (Figures 2 and 5A). Full-length recombinant ANAC, His_6-ANAC(1–317), was mostly insoluble. This was also the case for His_6-ANAC (1–138), lacking part of the conserved NAC domain (results not shown). In contrast, both His_6-ANAC(1–161) and His_6-ANAC (1–168), containing the conserved NAC domain, were soluble. Formation of secondary structure in recombinant His_6-ANAC (1–168) was confirmed by far-UV CD (Figure 5B). The minimum around 212 nm could be explained by β-strands, in accordance with secondary-structure predictions for the NAC domain (Figure 2). The unusual maximum around 228 nm and the low values between 190 and 200 nm can be explained by an N-terminal Pro-Pro-Gly motif in ANAC [35]. This motif tends to strongly influence the signals and is also present in the α-bungarotoxin [a neurotoxin found in the venom of the many-banded krait (*Bungarus multicinctus*)]. The spectrum of His_6-ANAC(1–168) showed features similar to those of the spectrum of α-bungarotoxin, which also contains a Pro-Pro-Gly motif and consists of β-strands linked by β-turns [36].

In the *in vitro* pull-down assay, His_6-ANAC(1–168) was allowed to bind MBP-RHA2a prior to addition of nickel-affinity matrix. SDS/PAGE and Western-blot analysis of the affinity-bound material showed that MBP-RHA2a(1–155) was recovered in the bound fraction, whereas MBP, also reacting with the antibody used for detection, was not (Figure 5C). This confirmed that RHA2a and ANAC interact and showed that the conserved NAC domain is sufficient for the interaction [29,31]. Thus, the NAC domain appears to define a RING-H2-binding domain that is different from previously defined RING-binding domains.

Specificity of RING-H2 interactions with ANAC

Quantitative two-hybrid analyses of the interaction between RHA2a and ANAC revealed an increase in β-galactosidase expression when truncated RHA2a(38–155) was used instead of full-length RHA2a(1–155) (Figures 4B and 6A). In contrast, no significant change in measurable β-galactosidase activity was detected, when RHA2a was truncated further in the RHA2a (77–155)–BD construct. This confirmed that the association between RHA2a and ANAC is via the core RING-H2 domain. The value of β-galactosidase activity obtained from co-transformation of the RHA2a(38–155)–BD and ANAC(1–317)–AD

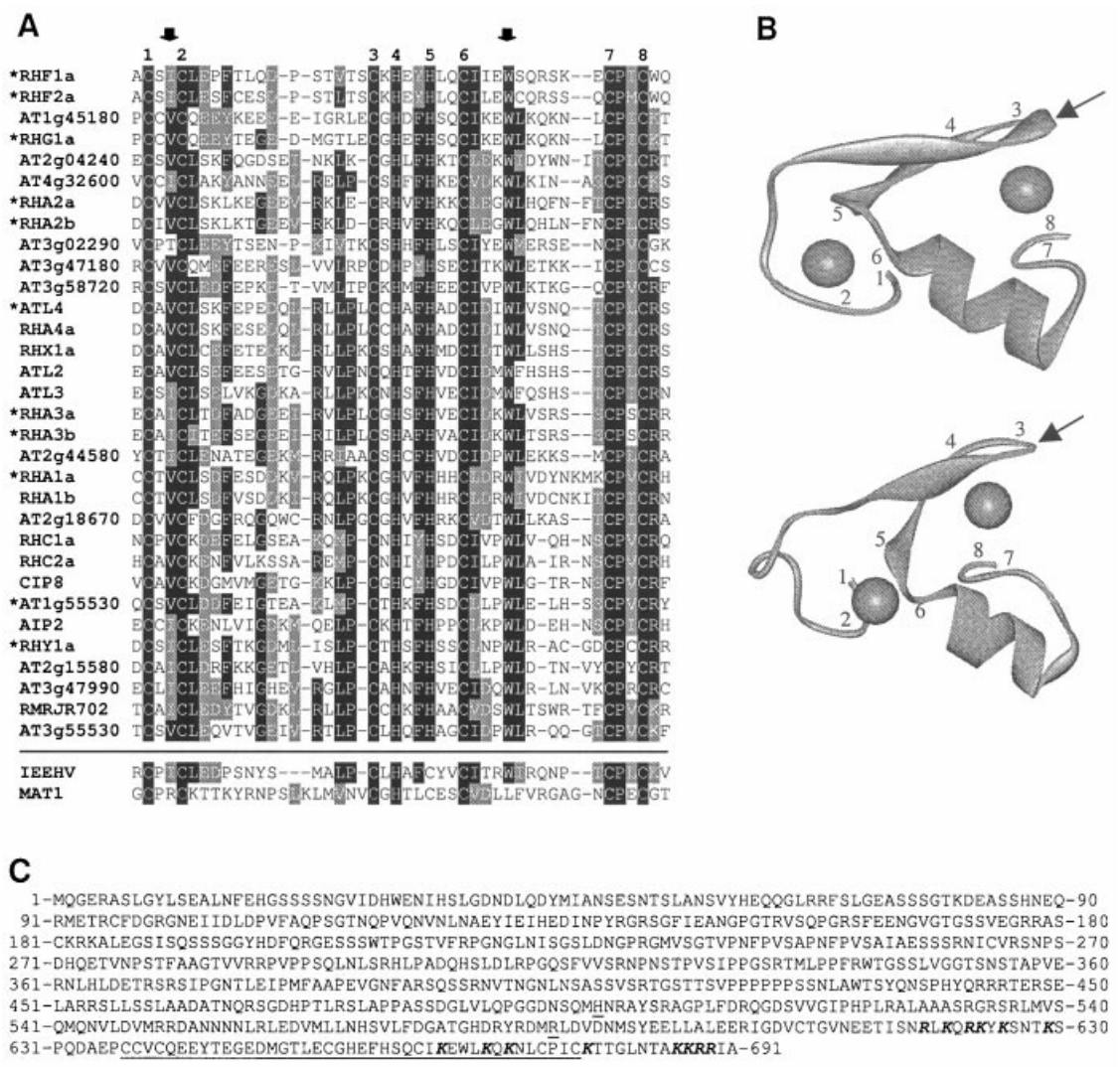

Figure 7 Conserved and variable regions of selected *Arabidopsis* RING-H2 fingers and amino acid sequence of RHG1a

(**A**) Alignment of the sequences of 32 *Arabidopsis* RING-H2 domains covering the structural diversity of the $CX_2CX_{14-15}CXHX_2HX_2CX_3WX_{6-8}CPXC$ RING-H2 domains (above the line). Metal ligands chelating the two zinc ions are numbered 1–8. Variable sequence regions are present between metal ligands 2 and 3 (region 1) and 6 and 7 (region 2). Proteins used for two-hybrid assays are marked with a star. Arrows show the positions corresponding to Trp^{408} and Ile^{383} in the E3 ligase c-Cbl. These amino acids are important for c-Cbl E2 specificity [38]. The sequences of the IEEHV and MAT1 RING-HC domains are shown below the line. (**B**) Ribbon diagram representation of IEEHV (top) [40] and MAT1 (bottom) [41] RING domains. Metal ligands chelating the two zinc ions are numbered 1–8. The amino acid position corresponding to Glu^{103} in RHA2a is a proline residue in IEEHV and a valine residue in MAT1 and is shown by an arrow. (**C**) Amino acid sequence of the predicted RHG1a protein. The RING-H2 domain is underlined; basic amino acids, including the predicted Lys-Lys-Arg-Arg NLS in the RING-H2 region, are shown in ***bold italics***, and the N-terminal amino acid in the RHG1a part of the two-hybrid fusion proteins RHG1a(584–691)–BD and RHG1a(50–691)–BD are underlined.

constructs was 17.5 ± 2.8 units. For comparison, the very strong control interactions between murine p53 and simian-virus-40 large T-antigen [37] produced β-galactosidase activities of 65.3 ± 6.2 units.

Most of the *Arabidopsis* RING-H2 domains contain the stringent $CX_2CX_{14-15}CXH\ X_2HX_2CX_3WX_{6-8}CPXC$ consensus sequence (Figure 7A) [17,26]. Sequence diversity in these domains is only pronounced in two short regions defined by metal ligands 2 and 3 and 6 and 7, as shown by alignment of sequences representing the structural diversity of the RING-H2 domains. cDNAs encoding divergent RING-H2 domains were selected to produce RING-H2–BD fusion proteins as baits for quantitative β-galactosidase two-hybrid interaction assays (Figure 7A; Table 1). Only short N- and C-terminal linker sequences were included in the constructs, since additional domains could influence the interactions [38].

RHA2b exhibits a high degree of sequence similarity to RHA2a, and its RING-H2 domain also interacted with ANAC (1–317) (Figure 6B). In contrast, the RING-H2 domain from RHA3a and RHA3b, also proteins with a high degree of mutual sequence similarity [17], did not interact with ANAC. Since Western analyses indicated that the BD fusion proteins were produced at similar levels, the ANAC interaction is likely to be dependent upon RING-H2 structure. The RHA1a(45–159)–BD fusion auto-activated in the system, as shown by β-galactosidase levels some 7-fold above background when the RHA1a (45–159)–BD and AD constructs were co-transformed. Co-transformation of RHA1a(45–159)–BD and ANAC(1–317)–AD

did not increase this level of β-galactosidase activity, suggesting that RHA1a does not interact with ANAC.

Directed two-hybrid assays also included RING-H2 domains from the RING-H2 proteins ATL4, RHF1a, RHF2a, RHG1a, RHY1a and At1g55530. Surprisingly, significant interaction was measured between RHG1a(584–691)–BD and ANAC (1–317)–AD. A weak interaction was also detected between RHF2a(1–106)–BD and ANAC(1–317)–AD. In contrast, interaction with ANAC was not detected for the RING-H2 domains from ATL4, RHF1a, RHY1a and At1g55530. The lack of interaction could be due to misfolded RING-H2 domains. However, the RING-H2–BD proteins were detected at similar levels, suggesting that they were soluble and folded. ATL4 (69–192)–BD, which did not interact with ANAC(1–317)–AD, interacted with the ubiquitin conjugase UBC10 (Figure 6D). On the basis of sequence properties, UBC10 is a likely E2 target for the ATL-like RING-H2 proteins [5]. The interaction between ATL4(69–192)–BD and ANAC(1–317)–AD also suggested that the RING-H2 domain of ATL4(69–192) was folded correctly.

Many of the RING-H2 domains contain a proline residue one or two amino acids before metal ligand 3 (Figure 7A). The RING-H2 domains from RHG1a, RHA2a, and RHA2b showed marked interaction with ANAC and contain an acidic amino acid at this position. To determine whether this difference is important for the differential binding of the RING-H2 domains to ANAC, Glu^{103} in RHA2a was converted into a proline residue and the mutated domain expressed from RHA2a(38–155; E103P)–BD (Figure 6C). Decreased interaction with ANAC (1–317)–AD was monitored for RHA2a(38–155; E103P)–BD compared with RHA2a(38–155)–BD. This decrease could be explained by disruption of the RING-H2 fold. However, this would most likely abolish the interaction. This was the case for RHA2a(38–155; C89S)–BD in which the RING-H2 fold was disrupted by a substitution of metal ligand 2 (Figure 6D). Because of difficulties with purification of RING-H2–BD fusion proteins from yeast, the effect of the $Glu^{103} \rightarrow Pro$ substitution on the RING-H2 fold was examined further using the corresponding recombinant protein. Zinc-binding stoichiometry was determined to probe the zinc-finger structure [39]. Purified MBP–RHA2a (1–155) and MBP–RHA2a(1–155; E103P) bound 1.8 and 1.9 mol of Zn^{2+}/mol of protein respectively, suggesting that the RING-H2 fold is intact in both proteins.

The decreased affinity of the mutated RHA2a(38–155; E103P) domain for ANAC(1–317) can then be explained by a change of the interaction surface. The amino acid corresponding to Glu^{103} in RHA2a maps to an exposed turn in the RING domain from both IEEHV [40] and the human MAT1 protein [41], which contain a proline and a valine residue respectively at this position (Figure 7B). The results pin-point the region defined by metal ligands 2 and 5 as an important part of the interaction surface. The RHA2a and RHG1a proteins show structural similarity in this region, including an acidic amino acid at the position corresponding to Glu^{103} in RHA2a and the acidic motif Glu-Gly-Glu-$^{Asp}/_{Glu}$. The RING-H2 domain from RHG1a interacted at least as strongly with ANAC as did the domain from RHA2a. Possibly, additional acidic residues in the region defined by metal ligand 2 and 3 in RHG1a may contribute to its interaction with ANAC.

To examine whether the interaction between RHG1a and ANAC involved regions outside the RING-H2 domain, RHG1a (502–691)–BD, encoding the RING-H2 and a 130-amino-acid N-terminal extension (Figure 7C), was co-transformed with ANAC(1–317)–AD. A decrease in measurable interaction indi cated that the region N-terminal to the RING-H2 domain attenuated the interaction detected in the two-hybrid system (Figure 6C). As described below this region contains a putative nuclear export signal (NES). Attempts to produce larger fragments of RHG1a in the yeast system were unsuccessful.

Cellular localization of ANAC, RHG1a and RHA2a

The RHG1a protein, predicted to contain 691 amino acids, contains no recognizable domains apart from the C-terminal RING-H2 domain (Figure 7C). The *RHG1a* gene is expressed in several tissues, including those expressing *ANAC* (Figure 3A). Both RT-PCR and Northern analyses suggested that *RHG1a* is also induced by ABA (Figures 3B and 3C). The expression profiles of *RHA2a* and *RHG1a* make them putative, physiologically relevant interaction partners.

To further analyse the physiological relevance of the biochemical interactions identified in the present study, the cellular localization of RHA2a, RHG1a and ANAC was examined. ANAC contains an almost complete bipartite nuclear localization signal (NLS) (Figure 2). RHG1a contains a basic NLS in the RING-H2 region that also contains additional basic amino acids, suggesting a role in nuclear targeting (Figure 7C). The presence of an NLS in both ANAC and RHG1a points to the nucleus as the location for their interaction.

To determine if the degenerate NLS in NAC can mediate import of the protein to nuclei, ANAC amino acids 1–317 were fused to the N-terminus of the *Escherichia coli GUS* gene [23]. ANAC(1–317)–GUS fusions were introduced into onion (*Allium cepa*) epidermal cells by particle bombardment [24]. This showed localization of ANAC(1–317)–GUS in both the nucleus and the cytoplasm in a pattern similar to that of a fusion containing the NLS of the maize (*Zea mays*) Opaque-2 bZIP transcription factor (O2) used as a positive control [24] (Figure 8A). The 68 kDa GUS protein was detected in the cytoplasm. RHG1a (614–691)–GUS contains the RING-H2 region with the basic NLS (Figure 7C) and was also mainly targeted to nuclei. Removal of the predicted NLS in RHG1a to generate RHG1a(614–685)–GUS resulted in a predominantly cytoplasmic localization of the fusion protein.

RHA2a(1–155)–GUS and RHA2a(38–155)–GUS, lacking the N-terminal hydrophobic region of RHA2a, were mainly detected in the cytoplasm (Figures 4B and 8A). However, further N-terminal deletion led to concentration of RHA2a(65–155)–GUS in the nucleus. This suggested that full-length RHA2a is either excluded or exported from the nucleus, and that an NLS mediates nuclear import of RHA2a(65–155)–GUS. RHA2a contains no classic NLS, but basic amino acids in zinc-finger domains can function as an NLS [42]. Several basic amino acids are present in the RHA2a RING-H2 domain. Lys^{110} and Lys^{111} are positioned between metal ligands 5 and 6, and they are likely to protrude from the RING-H2 domain. Two additional amino acids close to metal ligand 2 could contribute to a positively charged surface potentially involved in nuclear targeting (Figures 4B and 7B). To examine this, RHA2a Lys^{110} and Lys^{111} were changed to asparagine and glutamate residues respectively, and the localization of the mutant RHA2a(65–155; K110N,K111E)–GUS fusion protein was investigated. The double mutation abolished the nuclear concentration of the fusion protein. This could be due to removal of an NLS or to a disruption of the RING-H2 domain by the changes. Disruption of the RING-H2 fold is unlikely, since chemically different amino acids are allowed at corresponding positions in the RING-H2 domains (Figure 7A).

The presence of an NES in RHA2a could explain the difference in nuclear concentration of full-length and N-terminally truncated RHA2a. NESs have been identified in several well-characterized RING proteins, including the hdm2 oncoprotein [43],

A

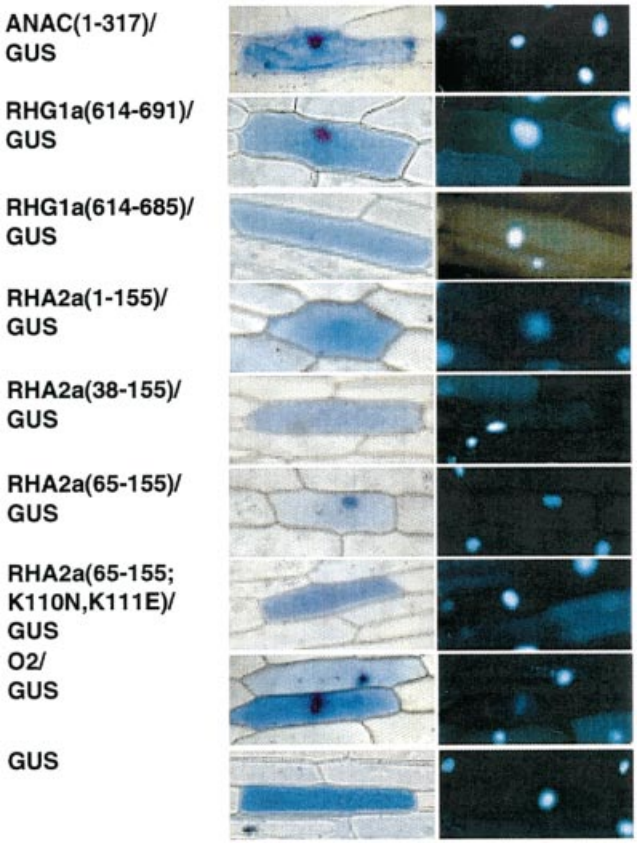

B

RHG1a	556	-	N	N	**L**	R	-	-	**L**	E	D	-	**V**	M	**L**	L	N
hdm2	188	-	I	S	**L**	S	-	-	**F**	D	E	S	**L**	A	**L**	C	V
RFP	198	-	Y	R	**L**	L	A	R	**L**	E	E	-	**L**	D	**L**	A	I
BRCA1	84	-	E	E	**L**	L	K	I	**I**	C	A	-	**F**	Q	**L**	D	T
RHA2a	57	-	A	N	**I**	I	V	-	**L**	A	D	Q	**L**	S	**L**	N	R
TFIIIA	328	-	D	P	**L**	P	V	-	**L**	E	N	-	**L**	T	**L**	K	S
RHA2a	43	-	P	N	**L**	P	-	-	**V**	D	D	-	**V**	S	**I**	A	S
Gle1	347	-	S	A	**L**	P	-	-	**L**	G	K	-	**L**	T	**L**	Y	L
Rev	73	-	L	Q	**L**	P	P	-	**L**	E	R	-	**L**	T	**L**	D	C
FMRP	428	-	D	Q	**L**	R	-	-	**L**	E	R	-	**L**	Q	**I**	D	E
Ran-BP1	178	-	E	K	**V**	A	E	K	**L**	E	A	-	**L**	S	**V**	K	E

Figure 8 Cellular localization of ANAC, RHG1a and RHA2a

(**A**) Localization of GUS, Opaque-2 NLS (O2)–GUS, ANAC–GUS, RHG1a–GUS and RHA2a–GUS reporter fusions in onion cells. Reporter genes are shown with amino acid numbers at the left. Histochemical staining of GUS activity in cells 24 h after particle bombardment (middle) and 4′,6-diamidino-2-phenylindole (‘DAPI’) staining of the same cells to identify nuclei (right) are shown. (**B**) Alignment of experimentally verified NESs in the RING-finger proteins hdm2 (human double minute 2), BRCA1 (breast cancer 1) and RFP [43–45] and in Ran-BP1 (Ran-binding protein 1), TFIIIA (transcription factor IIIA), Rev (anti-repression transactivator from HIV1), FMRP (fragile X mental retardation protein) and Gle1 (glossy spike 1) [46] and putative NES in RHA2a and RHG1a. Hydrophobic positions of importance to nuclear export are shown in **bold** [46].

BRCA1 [44] and the Ret finger protein (RFP) [45] (Figure 8B). NES elements consist of four or five hydrophobic amino acids within a region of approx. ten amino acids [46]. A computer-based search for NES elements suggested that they are frequent in *Arabidopsis* RING proteins [46] (results not shown). Putative NESs are also present in RHG1a (amino acids 556–567) and RHA2a (amino acids 57–70 and 43–54) (Figure 8B). These NESs are close to the signals that directed nuclear localization of GUS, in accordance with close spacing of NLS and NES in other RING proteins [43]. Two of the sequences (RHG1a amino acids 556–567 and RHA2a amino acids 43–54) contain a pair of acidic amino acids also present in NESs from the mammalian RING proteins (Figure 8B). In general, amino acids favoured in the region of the NES other than hydrophobic amino acids are glutamate and aspartate [46]. The function of the predicted NESs should be tested in *Arabidopsis* cells using green-fluorescent-protein reporter fusions.

DISCUSSION

Here we have identified the NAC transcription factor ANAC as a novel interaction partner for specific *Arabidopsis* RING-H2 domains. The N-terminal NAC domain is likely to form a β-sheet structure, e.g. a β-barrel or a β-sandwich (Figures 2 and 5B). For structures of this topology the loops between the β-strands often form the binding site for their target molecule, which, for NAC proteins, can be either proteins or DNA [31]. The ability to bind DNA and to auto-activate in the yeast two-hybrid system suggests that NAC proteins are nuclear-localized transcriptional activators. In keeping with this, both ANAC (1–317) and RHG1a(614–691) directed reporter GUS fusions to the nucleus. Further studies may show whether RHG1a is restricted to the nucleus or cycles between the nucleus and cytoplasm using a combination of its NLS and predicted NES (Figures 8A and 8B). Nucleocytoplasmic shuttling of RING proteins can serve a regulatory role in the control of transcriptional regulators [43]. In plants too, an increasing number of transcriptional regulators have been shown to be RING protein targets. In *Arabidopsis* the RING protein SINAT5 attenuates auxin signals by promoting ubiquitin-dependent proteolysis of NAC1 [15]. COP1 alone, or together with CIP8, may similarly regulate the level of the transcription factor HY5 [12,14]. The co-existence of ANAC(1–317)–GUS and RHG1a(614–691)–GUS in the nucleus and the induction of both the *ANAC* and the *RHG1a* genes by ABA (Figure 3C) suggest that RHG1a is a physiological regulator of ANAC.

The small RHA RING-H2 proteins contain a stretch of aliphatic amino acids at their N-termini that could form a transmembrane region (Figure 4B). However, transmembrane predictions are not consistent for the RHA proteins [17], and experimental data disfavour transmembrane anchoring of RHA2a. Thus recombinant MBP-RHA2a(1–155) was fully soluble, an unlikely property for a transmembrane protein. RHA2a (1–155)–BD interacted with ANAC(1–317)–AD in the two-hybrid system, suggesting that entrance of RHA2a(1–155)–BD into the nucleus was not obstructed by a transmembrane region. Finally, the RHA2a RING-H2 domain contains a signal that directed nuclear localization. The cellular localization pattern of RHA2a is in keeping with a physiologically relevant interaction with ANAC or another NAC protein. However, complex cellular localization patterns can be expected for both RING-H2 (Figure 8) and NAC proteins as part of their regulatory functions.

The results presented here demonstrate biochemical multi-specificity of interactions between the RING-H2 domains and ANAC. This, together with the recently identified interaction between the RING-HC protein SINAT5 and the NAC protein NAC1 [15], show variation in the interacting RING and NAC sequences. Whereas certain structural features such as Glu^{103} in RHA2a may be a key determinant for the interaction surface in the RING-H2 domains, variable sequence regions are likely to influence interaction affinity and specificity. One candidate region is the variable sequence region preceding Pro^{103} in RHA2a that

contains the acidic Glu-Gly-Glu-$^{Asp}/_{Glu}$ motif in both RHA2a and RHG1a (Figures 7A and 7B). Although hydrogen bonds and van der Waals contacts are important forces in protein complexes, electrostatic interactions could also influence the RING-H2 interactions with ANAC. However, high ionic strength in the 250 mM NaCl complex-formation buffer failed to resolve the *in vitro*-formed complex between MBP–RHA2a (1–155) and His_6-ANAC(1–168) (Figure 5C). This suggested that non-electrostatic interactions are also important for stabilizing the complex.

E3 ubiquitin ligase activity has been reported for several RING proteins, especially those with a RING-H2 domain [9]. In most cases the RING domain by itself is not sufficient for this activity, and RING-H2 proteins often function as part of multi-subunit complexes. Structural details of the single polypeptide E3 ligase c-Cbl in complex with the E2 ubiquitin-conjugating enzyme UbcH7 suggested that Trp^{408} and Ile^{383} in c-Cbl play a central role in determining the specificity of E3 for E2 [38]. These amino acids are chemically conserved in most of the *Arabidopsis* RING-H2 domains (Figure 7A), making them candidates as E2 interaction partners. The RING-H2 domain of *Arabidopsis* CIP8 was required, but was not sufficient, for its E3 ligase activity. Instead, CIP8 regions outside the RING-H2 domain most likely form the primary binding site for the E2 enzyme [12]. c-Cbl uses both its RING-HC and a neighbouring linker helix to bind UbcH7, but in this case the RING-HC domain forms the primary E2 binding site [38].

Although the RING domain in c-Cbl binds UbcH7, the variable sequence region 1, defined by metal ligands 2 and 3, is largely free to interact with another domain [38]. In the SCF complex, only part of the RING-H2 domain interacts with the Cullin subunit, which also allows other parts of the domain to interact with another protein such as an E2 enzyme [47]. Our results suggest that the RING-H2 domains in RHA2a and RHG1a form a primary binding site for ANAC, thereby representing a variation to the RING-domain interaction theme. However, the structurally simple RING-H2 proteins (Figure 1) could also contain binding sites for other proteins such as an E2 enzyme or an E3 multi-subunit component [48]. The ability of RHA2a and RHG1a to interact with such components should be tested. However, recent studies failed to show interaction between *Arabidopsis* Cullin1 and RHA2b in the yeast two-hybrid system, making the participation of RHA2b in an SCF-like complex less likely [49].

RHA2a and RHG1a also exhibit sequence similarities in variable sequence region 2, present between metal ligands 6 and 7 (Figure 7A). However, RHA2a is also distinct from most RING-H2 domains in this region by having an aromatic amino acid two positions before metal ligand 7. This has been inferred to be a key determinant for the plant homeodomain (PHD) zinc-finger fold [50]. The RING and PHD domains both have a cross-brace topology and very similar folds [50]. Although the metal-ligand pattern in the PHD domain (C_4HC_3) is distinct from that in the RING (C_3HC_4 and $C_3H_2C_3$) domains, the structural similarity creates a problem for *in silico* classification of the domains [26]. Because of the aromatic amino acid two positions before metal ligand 7 in the RHA2a and RHA2b zinc-finger domains, they were classified as PHD folds [26,50]. However, several criteria suggest that the zinc fingers in RHA2a and RHA2b represents a RING fold. The proteins show global structural similarity to the RHA RING-H2 proteins [17] suggestive of common evolutionary origin and overlapping functionality. The architectures of the simple RHA proteins are different from those of the PHD proteins, which are typically multidomain proteins. Furthermore, the sequence similarity between the *Arabidopsis* RING-H2 domains extends into variable sequence region 2 and includes the conserved, functionally important, tryptophan residue [17,38]. In the same region most of the PHD domains contain one or several proline residues, which most likely have an influence on the structure [50]. The interactions identified in the present study are therefore likely to represent interactions between typical RING-H2 domains and NAC proteins.

Even if minor structural variations are found between the RING-H2 domains of RHA2a and RHG1a, they may not be detectable in the interaction with their common protein partner ANAC. Structural determination of one of the abundant *Arabidopsis* RING-H2 domains is of interest and may help us to further understand and ultimately predict molecular interaction determinants and partner proteins. In any case, we have identified a novel interaction partner, the plant-specific ABA-inducible ANAC transcription factor, for the RING-H2 domain. This, together with the recent identification of the RING-HC protein SINAT5 as an interactor and modulator of NAC1 [15], suggests that RING–NAC interactions play a major role in plant biology. Further studies will reveal whether the RING-H2 proteins also regulate the activity of ANAC, either directly by binding of ANAC or by mediating ubiquitin-dependent degradation of ANAC.

This work was supported by grant number 9502825 from the Danish Research Council (to K.S.) and the John and Birthe Meyer Foundation (to F.M.P.). We thank Dr B. Kragelund for help with the CD experiments. The pACT cDNA library used for the two-hybrid screen was obtained from the *Arabidopsis* Biological Resource Center.

REFERENCES

1 Freemont, P. S., Hanson, I. M. and Trowsdale, J. (1991) A novel cysteine-rich sequence motif. Cell **64**, 483–484
2 Aravind, L. and Koonin, E. V. (2000) The U box is a modified RING finger – a common domain in ubiquitination. Curr. Biol. **10**, R132–R134
3 Kentsis, A. and Borden, K. L. B. (2000) Construction of macromolecular assemblages in eukaryotic processes and their role in human disease: linking RINGs together. Curr. Protein Peptide Sci. **1**, 49–73
4 Salinas-Mondragon, R. E., Garciduenas-Pina, C. and Guzman, P. (1999) Early elicitor induction in members of a novel multigene family coding for highly related RING-H2 proteins in *Arabidopsis thaliana*. Plant Mol. Biol. **40**, 579–590
5 Takai, R., Matsuda, N., Nakano, A., Hasegawa, K., Akimoto, C., Shibuya, N. and Minami, E. (2002) EL5, a rice *N*-acetylchitooligosaccharide elicitor-responsive RING-H2 finger protein, is a ubiquitin ligase which functions *in vitro* in co-operation with an elicitor-responsive ubiquitin-conjugating enzyme, OsUBC5b. Plant J. **30**, 447–455
6 Molnar, G., Bancos, S., Nagy, F. and Szekeres, M. (2002) Characterization of BRH1, a brassinosteroid-responsive RING-H2 gene from *Arabidopsis thaliana*. Planta **215**, 127–133
7 Borden, K. L. B. (2000) RING domains: master builders of molecular scaffolds? J. Mol. Biol. **295**, 1103–1112
8 Freemont, P. S. (2000) RING for destruction? Curr. Biol. **10**, R84–R87
9 Jackson, P. K., Eldridge, A. G., Freed, E., Furstenthal, L., Hsu, J. Y., Kaiser, B. K. and Reimann, J. D. R. (2000) The lore of the RINGs: substrate recognition and catalysis by ubiquitin ligases. Trends Cell Biol. **10**, 429–439
10 Potuschak, T., Stary, S., Schlogelhofer, P., Becker, F., Nejinskaia, V. and Bachmair, A. (1998) PRTI of *Arabidopsis thaliana* encodes a component of the plant N-end rule pathway. Proc. Natl. Acad. Sci. U.S.A. **95**, 7904–7908
11 Matsuda, N., Suzuki, T., Tanaka, K. and Nakano, A. (2001) Rma1, a novel type of RING finger protein conserved from *Arabidopsis* to human, is a membrane-bound ubiquitin ligase. J. Cell Sci. **114**, 1949–1957
12 Hardtke, C. S., Okamoto, H., Stoop-Myer, C. and Deng, X. W. (2002) Biochemical evidence for ubiquitin ligase activity of the *Arabidopsis* COP1 interacting protein 8 (CIP8). Plant. J. **30**, 385–394
13 von Arnim, A. G. and Deng, X. W. (1994) Light inactivation of *Arabidopsis* photomorpho-genic repressor COP1 involves a cell-specific regulation of its nucleocytoplasmic partitioning. Cell **79**, 1035–1045
14 Osterlund, M. T., Hardtke, C. S., Wie, N. and Deng, X. W. (2000) Targeted destabilization of HY5 during light-regulated development of *Arabidopsis*. Nature (London) **405**, 462–466

15 Xie, Q., Guo, H.-S., Dallman, G., Fang, S., Weissman, A. M. and Chua, N. H. (2002) SINAT5 promotes ubiquitin-related degradation of NAC1 to attenuate auxin signals. Nature (London) **419**, 167–170
16 Houvras, Y., Benezra, M., Zhang, H., Manfredi, J. J., Weber, B. L. and Licht, J. D. (2000) BRCA1 physically and functionally interacts with ATF1. J. Biol. Chem. **275**, 36230–36237
17 Jensen, R. B., Jensen, K. L., Jespersen, H. M. and Skriver, K. (1998) Widespread occurrence of a highly conserved RING-H2 zinc finger motif in the model plant *Arabidopsis thaliana*. FEBS Lett. **436**, 283–287
18 Altschul, S. F., Madden, T. L., Schaffer, A. A., Zhang, J., Zhang, Z., Miller, W. and Lipman, D. J. (1997) Gapped BLAST and PSI-BLAST: a new generation of protein database search programs. Nucleic Acids Res. **25**, 3389–3402
19 Letunic, I., Goodstadt, L., Dickens, N. J., Doerks, T., Schultz, J., Mott, R., Ciccarelli, F., Copley, R. R., Ponting, C. P. and Bork, P. (2002) Recent improvements to the SMART domain-based sequence annotation resource. Nucleic Acids Res. **30**, 242–244
20 Nakai, K. and Kanehisa, M. (1992) A knowledge base for predicting protein localization sites in eukaryotic cells. Genomics **14**, 897–911
21 Bujnicki, J. M., Elofsson, A., Fischer, D. and Rychlewski, L. (2001) Structure prediction metaserver. Bioinfomatics **17**, 750–751
22 Hunt, J. B., Neece, S., Schachman, H. K. and Ginsburg, A. (1984) Mercurial-promoted Zn^{2+} release from *Escherichia coli* aspartate transcarbamoylase. J. Biol. Chem. **259**, 14793–14803
23 van der Krol, A. R. and Chua, N.-H. (1991) The basic domain of plant B-ZIP proteins facilitates import of a reporter protein into plant nuclei. Plant Cell **3**, 667–675
24 Varagona, M. J., Schmidt, R. J. and Raikhel, N. V. (1992) Nuclear localization signal(s) required for nuclear targeting of the maize regulatory protein opaque-2. Plant Cell **4**, 1213–1227
24a Murashige, T. and Skoog, F. (1962) A revised medium for rapid growth and bioassay with tobacco tissue cultures. Physiol. Plant. **15**, 473–497
25 The *Arabidopsis* Genome Initiative. (2000) Analysis of the genome sequence of the flowering plant *Arabidopsis thaliana*. Nature (London) **408**, 796–815
26 Kosarev, P., Mayer, K. F. X. and Hardtke, C. S. (2002) Evaluation and classification of RING-finger domains encoded by the *Arabidopsis* genome. Genome Biol. **3**, 16.1–16.12
27 Souer, E., van Houwelingen, A., Kloos, D., Mol, J. and Koes, R. (1996) The no apical meristem gene of *Petunia* is required for pattern formation in embryos and flowers and is expressed at meristem and primordial boundaries. Cell **85**, 159–170
28 Aida, M., Ishida, T., Fukaki, H., Fujisawa, H. and Tasaka, M. (1997) Genes involved in organ separation in *Arabidopsis*: an analysis of the cup-shaped cotyledon mutant. Plant Cell **9**, 841–857
29 Xie, Q., Sanz-Burgos, A. P., Guo, H., Garcia, J. A. and Gutierrez, C. (1999) GRAB proteins, novel members of the NAC domain family, isolated by their interaction with geminivirus protein. Plant Mol. Biol. **39**, 647–656
30 Collinge, M. and Boller, T. (2001) Differential induction of two potato genes, *Stprx2* and *StNAC*, in response to infection by *Phytophthora infestans* and to wounding. Plant Mol. Biol. **46**, 521–529
31 Xie, Q., Frugis, G., Colgan, D. and Chua, N.-H. (2000) *Arabidopsis* NAC1 transduces auxin signal downstream of TIR1 to promote lateral root development. Genes Dev. **14**, 3024–3036
32 Petersen, M., Brodersen, P., Naested, H., Andreasson, E., Lindhart, U., Johansen, B., Nielsen, H. B., Lacy, M., Austin, M. J., Parker, J. E. et al. (2000) *Arabidopsis* map kinase 4 negatively regulates systemic acquired resistance. Cell **103**, 1111–1120
33 Kieber, J. J., Rothenberg, M., Roman, G., Feldmann, K. A. and Ecker, J. R. (1993) CTR1, a negative regulator of the ethylene response pathway in *Arabidopsis*, encodes a member of the raf family of protein kinases. Cell **72**, 427–441
34 Skriver, K. and Mundy, J. (1990) Gene expression in response to abscisic acid and osmotic stress. Plant Cell **2**, 503–512
35 Bhatnagar, R. S. and Gough, C. A. (1996) Circular dichroism of collagen and related polypeptides. In Circular Dichroism and the Conformational Analysis of Biomolecules (Hill, G. D., ed.), pp. 183–199, Plenum Press, New York
36 Wu, S.-H., Chen, C.-J., Tseng, M.-J. and Wang, K.-T. (1983) The modification of α-bungarotoxin by digestion with trypsin. Arch. Biochem. Biophys. **227**, 111–117
37 Li, B. and Fields, S. (1993) Identification of mutations in p53 that affect its binding to SV40 T antigen by using the yeast two-hybrid system. FASEB J. **7**, 957–963
38 Zheng, N., Wang, P., Jeffrey, P. D. and Pavletich, N. P. (2000) Structure of a c-Cbl–UbcH7 complex: RING domain function in ubiquitin-protein ligases. Cell **102**, 533–539
39 Berg, J. M. and Godwin, H. A. (1997) Lessons from zinc-binding peptides. Annu. Rev. Biophys. Biomol. Struct. **26**, 357–371
40 Barlow, P. N., Luisi, B., Milner, A., Elliott, M. and Everett, R. (1994) Structure of the C3HC4 domain by ^{1}H-nuclear magnetic resonance spectroscopy. A new structural class of zinc-finger. J. Mol. Biol. **237**, 201–211
41 Gervais, V., Busso, D., Wasielewski, E., Poterszman, A., Egly, J.-M., Thierry, J.-C. and Kieffer, B. (2001) Solution structure of the N-terminal domain of the human TFIIH MAT1 subunit. J. Biol. Chem. **276**, 7457–7464
42 Perander, M., Bjørkøy, G. and Johansen, T. (2001) Nuclear import and export signals enable rapid nucleocytoplasmic shuttling of the atypical protein kinase C λ. J. Biol. Chem. **276**, 13015–13024
43 Roth, J., Dobbelstein, M., Freedman, D. A., Shenk, T. and Levine, A. J. (1998) Nucleo-cytoplasmic shuttling of the hdm2 oncoprotein regulates the levels of the p53 protein via a pathway used by the human immunodeficiency virus rev protein. EMBO J. **17**, 554–564
44 Rodriguez, J. A. and Henderson, B. R. (2000) Identification of a functional nuclear export sequence in BRCA1. J. Biol. Chem. **275**, 38589–38596
45 Harbers, M., Nomura, T., Ohno, S. and Ishii, S. (2001) Intracellular localization of the Ret finger protein depends on a functional nuclear export signal and protein kinase C activation. J. Biol. Chem. **276**, 48596–48607
46 la Cour, T., Gupta, R., Rapacki, K., Skriver, K., Poulsen, F. M. and Brunak, S. (2003) NESbase version 1.0: A database of nuclear export signals. Nucleic Acids Res. **31**, 393–396
47 Zheng, N., Schulman, B. A., Song, L., Miller, J. J., Jeffrey, P. D., Wang, P., Chu, C., Koepp, D. M., Elledge, S. J., Pagano, M. et al. (2002) Structure of the Cul1-Rbx1-Skp1-F boxSkp2 SCF ubiquitin ligase complex. Nature (London) **416**, 703–709
48 Gray, W. M., Hellmann, H., Dharmasiri, S. and Estelle, M. (2002) Role of the Arabidopsis RING-H2 protein RBX1 in RUB modification and SCF function. Plant Cell **14**, 2137–2144
49 Lechner, E., Goloubinoff, P., Genschik, P. and Shen, W. H. (2002) A gene trap dissociation insertion line, associated with a RING-H2 finger gene, shows tissue specific and developmental regulated expression of the gene in *Arabidopsis*. Gene **290**, 63–71
50 Capili, A. D., Schultz, D. C., Rauscher, F. J. and Borden, K. L. B. (2001) Solution structure of the PHD domain from the KAP-1 corepressor: structural determinants for PHD, RING and LIM zinc-binding domains. EMBO J. **20**, 165–177

Received 16 July 2002/9 December 2002; accepted 20 December 2002
Published on the Internet 25 March 2003, DOI 10.1042/BJ20021123